https://ntrs.nasa.gov/search.jsp?R=19850010715 2020-03-20T20:20:54+00:00Z

3 1176 01351 7991

NASA Contractor Report 172547

NASA-CR-172547
19850010715

EVALUATION OF FAILURE CRITERION FOR GRAPHITE/EPOXY FABRIC LAMINATES

R. C. TENNYSON AND G. E. WHARRAM

UNIVERSITY OF TORONTO
Institute for Aerospace Studies
Toronto, Ontario, Canada

Grant NSG-7409

February 1985

LIBRARY COPY

LANGLEY RESEARCH CENTER
LIBRARY, NASA
HAMPTON, VIRGINIA

National Aeronautics and Space Administration

Langley Research Center
Hampton, Virginia 23665

TABLE OF CONTENTS

N85-19025#

1.0 INTRODUCTION

In the construction of laminated composite structures, the fabricator can select from a wide range of composite material systems. Generic materials such as glass, graphite and aramid fibers (such as Kevlar™) are available both in the "dry" and "prepreg" forms, to satisfy a diverse set of design requirements. Depending on the application, one can fabricate components by filament or tape winding methods, or by laying up a configuration utilizing commercial prepreg materials which meet relatively stringent quality control criteria (in terms of resin/fiber content, volatile content as well as specified physical/mechanical properties). In the case of prepreg systems, the manufacturer has the option of choosing between unidirectional and woven fabric formats. However, when one considers manufacturing and design requirements, it is often more cost-effective to utilize the woven fabric system.

One major problem area that continues to plague the design engineer is the selection of suitable strength criteria for composite laminates, regardless of the material system and manufacturing process being used. In aerospace construction, one usually encounters relatively thin-walled structures and thus, to a first approximation, a plane stress state can be assumed to exist for preliminary design purposes. However, it is becoming increasingly evident that in many instances, three-dimensional stress effects must be considered, particularly in the vicinity of free edges (associated with joints, cutouts, fasteners, etc.). Indeed, such effects can lead to delamination and/or crack initiation which are of major concern to the analyst. Regardless of the stress state, the requirements for lamina and overall structural failure criteria still persist. The most desirable failure model is one which can provide conservative maximum load estimates of reliable accuracy. However, the model must not be so conservative that

it jeopardizes the design itself in terms of increasing the weight needlessly. On the other hand, it should be relatively operationally easy to employ, and not be dependent on the development of such an extensive data base using complex and expensive test procedures that the user shuns its application. One might comment that the presence of local stress concentrations (due to cracks, free edges, holes, etc.) does not influence the form of a lamina strength criterion. Rather, such considerations can be taken into account in the formulation of the stress analysis and the failure criterion one adopts for the whole laminate. For example, if one is performing a finite element analysis, including three-dimensional stress terms, failure is determined not only by the lamina failure model, but equally as important, by the laminate failure model one assumes.

Lamina failure models can essentially be grouped into three categories of increasing operational complexity. The simplest approach is to design to maximum stress or strain (which are not equivalent criteria). Unfortunately, these models lead to substantial "over-estimates" of strength in the "corner" regions of the failure surface envelope. The next class of models are those which approximate the failure surface by quadratic polynomials of different forms. Many variations of quadratic models can be found in the literature, including ones which define the surface using different functions for each quadrant. Again, it has been demonstrated that, for certain load cases, quadratic formulations can overestimate strength as well (Ref. 1). In some instances, such as biaxial loading, the quadratic criterion can under predict strength by as much as 30%-40% (Ref. 2). The third category of failure criteria is termed "higher order models", the most common one of which is the "cubic" polynomial (Refs. 1, 2, 3). It should be noted that all of the above mentioned formulations represent approximations encompassed by the general "tensor polynomial"

criterion advocated in Ref. 3. The one feature that is common to all of these lamina failure models is that they represent a phenomenological, macro-mechanics approach to predicting lamina failure. They all attempt to describe the real failure surface in stress (or strain) space. Table 1 presents a summary of the test data and interaction strength parameters that one would require for each classification of failure model. It becomes quite apparent that the higher order cubic model demands more baseline strength data. This of course raises the question as to whether or not the additional complexity (and cost) is warranted. Although it has been shown that for laminates constructed from unidirectional prepregs that the higher order model is required for certain regions of stress space, recent work (Ref. 4) on NARMCO-5208-K285 Kevlar® 49 fabric (a 4 harness satin weave, over 3, under 1) demonstrated that the quadratic formulation was quite satisfactory for predicting strength, providing the interaction parameter $F_{12} = 0$. This work has now been extended to include a graphite/epoxy fabric prepreg - NARMCO Rigidite 5208-WT300 in the form of a plain weave (over 1, under 1). The major objective of this report is to present and utilize the relevant stress-strain data and strength measurements to formulate a failure model.

2.0 MATERIAL DESCRIPTION

The woven fabric prepreg used in this second phase of the program (see Ref. 4) was Narmco Rigidite 5208-WT300, a plain weave (over 1, under 1) of UCC Thornel 300 graphite fibers impregnated with Narmco 5208 resin. The angle between the warp and fill direction fibers was found to vary by up to 5 degrees. As was done with the Kevlar weave material studied in phase 1 of the program (Ref. 4), the graphite weave material was straightened prior to curing. This was necessary in order

to obtain the material properties in the fiber directions without the modulus and strength reductions which occur due to fiber misalignment.

3.0 MANUFACTURING AND TEST PROCEDURES

3.1 Manufacture of Specimens

Both tubular and flat specimens were manufactured using the Narmco standard autoclave cure cycle. Since the graphite weave prepreg had only 39% resin content before curing, no bleeder material was used during specimen fabrication. The resulting specimens had a cured thickness of 0.0074" per ply. The specimens were cured at 350^{o}F with 90 psi pressure, although the optional post-cure was not performed since all testing was conducted at room temperature.

After fabrication, the specimens were cut to the proper size by using a high speed abrasive disk. The apparatus employed for cutting the flat specimens is shown in Figure 1. Tubular specimens were cut by mounting them on a lathe and using an air powered cutting disk as shown in Figure 2.

One of the problems encountered with Kevlar prepreg fabric (as reported in Ref. 4) was fill-direction fiber misalignment, as noted earlier. Thus, it was decided to straighten the graphite fibers prior to each specimen layup. This was accomplished by clamping one edge of the material and then pulling the material until the fill direction fibers were straight. Care must be taken to ensure that the warp direction fibers remain straight during this process. This procedure was successful in providing specimens with fibers straight in both directions and nearly orthogonal to each other. However, it was found to work well only for small sections of material and is not suggested for large scale work. It must be emphasized that pre-straightening and alignment are necessary to obtain optimum properties of the material in its correct

orientation. Only in this way can one achieve maximum strength (and stiffness) for various load conditions and ply orientations.

3.2 Tension Tests

The specimens used in the tension tests were 3 ply, 2" wide by 6" long, flat coupons. Aluminum end tabs 2" wide × 1 1/2" long × 1/8" thick were attached to both ends using American Cynamid FM300 adhesive film. The end tabs were held in place while curing, with the potting grip fixture shown in Figure 3. The film adhesive was cured at 350°F for one hour.

Strain gauges were then applied to the specimen to measure both the axial and transverse strains. Gauges were used on both sides of the specimen to measure the amount of bending that was present during testing.

Each specimen was placed in a set of end grips which were mounted in a Tinius Olsen, 4 screw, electrically driven test machine. A set of gimballed end fittings were also used to minimize any bending moments from being applied to the specimen. The specimen grips are shown in the testing machine in Figure 4.

Load and strain readings were taken using an Optilog data acquisition system and stored in an Apple II plus microcomputer. These results were then employed to calculate the tensile moduli E_{11T} for the 0° samples, E_{22T} for the 90° samples and the Poisson ratio's ν_{12} and ν_{21}. These tests also provided the 0° strength (X), 90° strength (Y) and ultimate strains, ε_{1ult_T} and ε_{2ult_T}.

3.3 Compression Tests

The specimens used for compression testing were 10 plies thick, 0.75" wide by 3.5" long. Aluminum end tabs .75" wide by 1.5" long by 1/16" thick were bonded on with FM300 adhesive film and cured at 350° F for one hour.

The specimens were then mounted in an IITRI-type compression fixture as shown in Figure 5. The test fixture was subsequently placed in the Tinius Olsen testing machine and the load applied through a hardened steel loading bar.

Strain gauges were mounted on both sides of the specimen to measure axial strains. Due to the specimen size, transverse strain measurements were not taken. It is very important to have gauges on both sides of the specimen since they can be used to determine whether failure occurs due to buckling, and to calculate the amount of bending stress applied to the coupon. These considerations are very important in compression testing, while not as significant in tension tests.

As with the tension tests, the load and strain data were collected using the Optilog and Apple II microcomputer. From this data, the compressive moduli E_{11C} and E_{22C} were calculated as well as the strengths X'(0°), Y'(90°) and the maximum strains, ε_{1ult_C} and ε_{2ult_C}.

3.4 Torsion Tests

The torsion tests were performed using tubular specimens, 6 plies thick, 2" in diameter and 6" long (based on results obtained in Ref. 4). The tubes were bonded into circular aluminum end pots using Hysol 6175 resin and 3561 hardener. They were centrally mounted and aligned orthogonal to the base of both end pots. The tubes were positioned in a torsion fixture attached to the Tinius Olsen, which served as a rigid base. Torque loading was applied by two hydraulic pistons which were connected to a circular plate, fastened to the top of the tube. The pistons were then pressurized by a hand operated pump. A view of the test setup is shown in Figure 6.

A pressure transducer was connected to the hydraulic pistons, thus providing the data necessary to calculate the applied torque. Strain gauges were bonded on the specimen at ± 45° to the tube's longitudinal axis. These

gauges provided the shear strain present in the sample. The pressure and strain data were collected using the same data acquisition system described earlier and used to calculate the material shear modulus G_{12}. The other data resulting from these tests are the shear strength (S) and the maximum shear strain (γ_{ult}).

3.5 Biaxial Load Tests

In order to calculate the interaction parameters for the failure theory, it was necessary to perform some biaxial loading tests. For woven fabric materials, internal pressure tests on 0° or 90° tubes will provide the proper stress state. If one considers the cubic form of the failure equation, then three points are required for solving F_{12}, F_{112} and F_{122}. Three test configurations were selected; 0^0 and 90^0 internal pressure, and 0^0 internal pressure with axial compression.

The specimens fabricated for these tests were 4 ply, 2" diameter by 6" long tubes. The tubes were made with a continuous wrap of prepreg to obtain all four plies. This was done because failure occurs predominantly from the failure of the hoop direction fibers. It was also necessary to reinforce the tube near the end fittings, to prevent premature failure from occurring there.

The tubes, once manufactured, were again potted into aluminum end fittings using Hysol 6175 and 3561. The end fittings were connected to an air operated hydraulic pump and the tube filled with oil. In this procedure, the pump was used only to pressurize a reservoir. Subsequently, by opening a valve between the reservoir and the tube, the pressure in the tube was increased slowly until failure occurred. The pressure test setup is shown in Figures 7 and 8. Axial and circumferential gauges were employed to verify the tube stiffness and to record the strains at failure. In addition, a pressure transducer was placed at the inlet to the specimen,

thus permitting the pressure and strain values to be recorded as before. At the same time, they were monitored on an x-y plotter to provide control of the loading rate.

For the combined compression-pressure test, the same procedure as above was used, only the tube was placed in the Tinius Olsen below a loading platen. The specimen was then subjected to a specific ratio of pressure to compressive loading so that the net axial stress applied to the tube was compressive. This process was also controlled by monitoring the pressure transducer and the load, all on an x-y plotter, and then following a preset loading curve. Strain values were recorded in the same manner as the pressure tests.

The results from these tests yielded ultimate failure pressures which defined the stress state at failure $\sigma_{1_{ult}}$, $\sigma_{2_{ult}}$ and the strain state at failure $\varepsilon_{1_{ult}}$, $\varepsilon_{2_{ult}}$.

To determine the shear interaction terms F_{166} and F_{266}, a combined tension-torsion test was performed. The method of torsion loading was identical to that described previously, with the addition of a tensile load applied simultaneously. As with the pressure-compression test, the loading followed a prescribed ratio of tensile load to torque. The test facility is shown in Figure 9. Both 0° and 90° tubes were investigated to calculate the two interaction terms. The specimens used were 6 ply, 2" diameter tubes, 6" long and were mounted in the same manner as the torsion test samples.

A further verification of the failure theory can be obtained by performing internal pressure tests on $\pm\theta$ symmetric balanced tubes. This configuration provides simultaneous stresses in both fiber directions and shear stresses as well. The tests were conducted on 4 ply tubes with $\pm 45^{0}$ and $\pm 30^{0}$ orientation. Comparisons can then be made between the predicted and experimental failure stresses and strains.

4.0 DISCUSSION OF TEST RESULTS

4.1 Tension

The results of the tension tests are presented in Table 2 for the 0^o and 90^o specimens. Sample stress-strain curves are also shown in Figures 10 and 11 for the 0^o and 90^o tests, respectively. Due to the nature of the woven material it was expected that the material properties would be essentially equal in the two fiber directions. As can be seen in Table 2 and Figures 10 and 11, this is true for tensile loading.

The tensile strengths are, for the 0^o direction X = 65.8 ksi and for the 90^o direction, Y = 70.0 ksi, giving an average value of 67.9 ksi. From Figures 10 and 11, the tensile modulus is linear to failure with the values being for the 0^o direction, $E_{11} = 9.92 \times 10^6$ psi and for the 90^o direction $E_{22} = 10.20 \times 10^6$ psi, thus giving an average value of 10.06×10^6 psi. The strain to failure (ε_{ult}) is for the 0^o direction, 0.67% and for the 90^o direction 0.69%, for an average value of 0.68%. The Poisson ratio is the same for both directions and has a value of $\nu_{12} = 0.065$.

4.2 Compression

The compression test results and stress-strain curves are presented in Table 3(a) and Figure 12 for the 0^o tests and in Table 3(b) and Figure 13 for the 90^o samples.

The compressive strengths are for the 0^o direction, X' = 66.2 ksi, for the 90^o direction Y' = 67.1 ksi, for an average value of 66.7 ksi. The compressive moduli are $E_{11} = 7.62 \times 10^6$ psi and $E_{22} = 8.24 \times 10^6$ psi, giving an average compressive modulus of 7.93×10^6 psi. The ultimate strains are 0.89% and 0.86% for the 0^o and 90^o directions respectively, with an average $\varepsilon_{ult} = 0.87\%$. From Figures 12 and 13 it can be seen that the compressive modulus is linear to failure, unlike the Kevlar weave material previously studied (see Ref. 4) which was very non-linear. Since the bending

stress in the specimen (shown as the difference between the two lines in Figures 12 and 13) was small, it was not included in the calculation of the stress at failure and thus the average stress in the specimen was used.

4.3 Torsion

The shear stiffness and strength data resulting from torsion loading of 0^o and 90^o tubes are presented in Tables 4(a) and 4(b), respectively. Typical stress-strain curves are also given in Figures 14 and 15 for the 0^o and 90^o tests, respectively.

As can be seen from Tables 4(a) and 4(b), the results from the 0^o and 90^o torsion tests are very similar, which verifies the assumption that the material behaves identically under 'positive' and 'negative' shear loading. The shear strength is 17.2 ksi for the 0^o direction and 17.3 ksi for the 90^o direction. Figures 14 and 15 show that the shear response is non-linear. As was done with the Kevlar weave material (Ref. 4), shear modulus was calculated based on the average slope up to 50% of the ultimate shear stress. The resulting shear moduli are 0.74×10^6 psi and 0.75×10^6 psi for the 0^o and 90^o directions, respectively, giving an average value of $G_{12} = 0.745 \times 10^6$ psi. The strain to failure is 5.85% and 5.45% for the 0^o and 90^o directions, respectively, for an average shear strain at failure of $\gamma_{ult} = 5.65\%$.

A summary of the average material properties for the NARMCO 5208-WT300 graphite/epoxy fabric prepreg as determined in this investigation is presented in Table 5. The strength results shown are sufficient to calculate the principal strength parameters. However, the presence of interaction effects must now be determined from combined loading tests.

5.0 BIAXIAL LOAD TESTS

5.1 Internal Pressure Tests

The stresses and strains at failure resulting from internal pressure

tests on 0^0 and 90^0 tubes are presented in Tables 6 and 7. One of the problems experienced in these tests was premature failure occurring where the second ply overlaps the first. Such failures were consistently lower than those observed on specimens which failed away from the overlap area. It is conjectured that premature failure probably occurred due to a localized stress concentration at the overlap where the fibers were bent. A summary of these premature failure tests is given in Table 7. Also shown is the pressure load ratio based on the mean value of the tests contained in Table 6 and those failure pressures observed in the overlap region. Using the average factor shown, the unadjusted 'failure stresses' were 'corrected' to account for the 'overlap effect' and are summarized in Table 8. These values were not used in calculating the strength properties (i.e. interaction terms) but provided additional data points to compare with the predicted failure surfaces.

The failure stresses for the 0^0 and 90^0 pressure tests are plotted in Figure 16, including the adjusted data as well. This graph shows the experimental failure stresses in the σ_1-σ_2 plane (i.e. σ_6=0), as well as two different theoretical predictions which will be discussed later.

5.2 Pressure-Compression Tests

Achieving 'acceptable' failure conditions in this test configuration was very difficult due to the sensitivity of the compression failure mode to imperfections in the laminate. The 'best' failure achieved was one which occurred along the ply overlap and is thus included in Table 8. The adjusted failure stresses shown were used only for comparison with theoretical strength predictions and were not employed to calculate any of the interaction strength parameters.

5.3 Tension-Torsion Tests

The results from these tests are also presented in Table 6, and are

plotted in Figure 17 for the 0^o samples and in Figure 18 for the 90^o samples. A discussion of the failure curves and their comparisons with test data will be given later.

5.4 Internal Pressure Tests on ±θ Symmetric Balanced Tubes

Internal pressure tests on ±θ, symmetric balanced tubes yield non-zero values of σ_1, σ_2 and σ_6, thus providing a good test configuration for comparison with theoretical predictions. Tests were performed on 4 ply, $\pm 45^o$ and 4 ply, $\pm 30^o$ tubes, and the resulting failure stresses listed in Table 6. These results together with 0^o and 90^o pressure test data are plotted in Figure 19, which shows failure pressure vs. ply angle for internal pressure loading.

6.0 FAILURE MODEL FOR WOVEN FABRIC LAMINATES

The reader is referred to Tables 5 and 6 which contain the relevant orthotropic material properties and strength data required to formulate a failure model. Based on these results, one can readily calculate the strength parameters associated with the quadratic and cubic tensor polynomial failure criteria. For reference purposes, the general form of this criterion is (Ref. 3), Tsai ; Wu

$$F_i\sigma_i + F_{ij}\sigma_i\sigma_j + F_{ijk}\sigma_i\sigma_j\sigma_k + \ldots = f(\sigma) \begin{cases} < 1 \text{ no failure} \\ = 1 \text{ failure} \\ > 1 \text{ exceeded failure} \end{cases} \quad (1)$$

for i, j, k = 1...6. F_i, F_{ij} and F_{ijk} are strength tensors of the 2nd, 4th and 6th rank, respectively. For the case of a plane stress state, Eq. (1) reduces to (see Refs. 1, 2, 3),

$$F_1\sigma_1 + F_2\sigma_2 + F_{11}\sigma_1^2 + F_{22}\sigma_2^2 + F_{66}\sigma_6^2 + 2\,F_{12}\,\sigma_1\sigma_2 + 3\,F_{112}\sigma_1^2\sigma_2 +$$

$$3\,F_{122}\sigma_1\sigma_2^2 + 3\,F_{166}\sigma_1\sigma_6^2 + 3\,F_{266}\sigma_2\sigma_6^2 = 1 \qquad (2)$$

if one retains cubic terms. The principal strength parameters are defined by,

$$F_1 = \frac{1}{X} - \frac{1}{X'}, \quad F_2 = \frac{1}{Y} - \frac{1}{Y'}, \quad F_{11} = \frac{1}{XX'}, \quad F_{22} = \frac{1}{YY'}, \quad F_{66} = \frac{1}{S^2} \qquad (3)$$

where X, Y define tensile strengths in the fiber (or warp) and matrix (or fill) directions, respectively; X', Y' define the corresponding compressive strengths and S is the shear strength measured in the principal material axes plane. The interaction terms include F_{12}, F_{112}, F_{122}, F_{166} and F_{266}. The corresponding quadratic form of Eq. (2) is,

$$F_1\sigma_1 + F_2\sigma_2 + 2\,F_{12}\sigma_1\sigma_2 + F_{11}\sigma_1^2 + F_{22}\sigma_2^2 + F_{66}\sigma_6^2 = 1 \qquad (4)$$

In many cases, F_{12} is taken equal to zero, although many authors select $F_{12} = -\frac{1}{2}(F_{11}F_{22})^{1/2}$ to ensure a "closed" failure surface in stress space. The consequences of this assumption will be made clear later as it relates to the analysis of fabric laminates, as previously discussed in Ref. 4.

Based on Eq. (3), one calculates the principal strength parameters from the data listed in Table 5. Furthermore, using the biaxial failure data presented in Table 6 and using Eq. (2), one can then solve for the interaction parameters noted above. Table 9 provides a summary of the strength parameters required for a cubic model representation of the failure surface. Plots of the three planes $\sigma_1 - \sigma_2$, $\sigma_1 - \sigma_6$ and $\sigma_2 - \sigma_6$

have been mentioned earlier, and one can again refer to Figs. 16-18 to compare the various solutions.

Examining first the σ_1-σ_2 plane (Figure 16), it was found that the 'best' solution was obtained from the quadratic model (with $F_{12} = F_{122} = F_{112} = 0$). As was found with the Kevlar weave material in Ref. 4, the theoretical quadratic value of $F_{12} = -\frac{1}{2}(F_{11} F_{22})^{\frac{1}{2}}$ tends to greatly overestimate the lamina strength and should not be used.

The effect of the remaining cubic terms F_{166} and F_{266} is shown in Figures 17-19. It is interesting to note that the difference between the cubic and quadratic solutions is less than 30% with the quadratic solution being conservative for tensile loading, but over-predicting the cubic solution for compressive loading. From Figure 19 it can be seen that the terms F_{166} and F_{266} are significant only over the region $30^{\circ}<\theta<60^{\circ}$ for internal pressure loading. The effect of neglecting these terms will be discussed in the following section.

7.0 USE OF CUBIC MODEL FOR DESIGN PURPOSES

It has been demonstrated both in Ref. 4 and in this study that for the two fabric prepreg materials studied, a quadratic model with $F_{12} = 0$ provides reasonably good agreement with the test data obtained. However, a note of caution should be issued at this point because it is not known to what extent the orthotropic fabric strengths must differ before one is faced with the requirement of using a higher order failure model. One does know that, for example, laminae formed from unidirectional prepregs where the tensile strength ratios $(\frac{X}{Y})$ are of the order of 20, the cubic model works best. Clearly a transition must take place as $X/Y \rightarrow 1.0$.

As was done in Ref. 4, one can at least present the cubic model predictions in a form that alerts the analyst to regions of stress

space where the quadratic model 'over' or 'under' estimates lamina strength for a given material system.

It is generally acknowledged that one of the major problems in the utilization of a higher order failure criterion (such as the cubic model) is the difficulty involved in evaluating the additional strength parameters(see Ref. 2 for example). For the design engineer and analyst, if the data are not available, one simply cannot apply the criterion and recourse to simpler models is necessary. In this section, an attempt has been made to reduce the known cubic model strength data to an "operationally easier" form for the graphite/epoxy fabric studied. As a reference basis, it will be assumed that the minimum strength data available to the engineer include unidirectional measurements of the fiber and matrix dominated tensile and compressive strengths (i.e.: X, X', Y, Y') together with the shear strength (S) in the principal material axes plane (see Table 5). Thus, for a plane stress state, one can employ the quadratic model [Eq. (4)] with $F_{12} = 0$.

If one now considers the difference in solutions between the cubic and quadratic models for given values of the load vector (defined by the co-ordinates R, θ, ϕ in $\sigma_1 - \sigma_2 - \sigma_6$ stress space - see Fig. 20), "design factors" can then be calculated for "correcting" the quadratic strength predictions. The curves shown in Fig. 21 were generated for the graphite weave material discussed in this report. The application of these curves requires knowledge of the ply stresses throughout the laminate. One can then calculate R, θ, ϕ from

$$R = (\sigma_1^2 + \sigma_2^2 + \sigma_6^2)^{1/2}$$
$$\theta = \tan^{-1}(\sigma_2/\sigma_1) \qquad (5)$$
$$\phi = \tan^{-1}(\sigma_6/R)$$

for each ply. Note that the restricted range of ϕ angles shown is due to the very small strength values associated with σ_6 (i.e.: S) relative to the fiber strengths (X, X'). These curves can be regarded as providing non-dimensional "correction factors" and thus one does not need to evaluate the interaction terms. Again, a note of caution is in order since only a limited number of materials have been investigated and clearly more data on other unidirectional prepregs and weave materials would be valuable before generalizations about the application of these curves can be made.

The main advantage of this form of solution presentation is that the design engineer can determine if indeed his stress state puts him into a conservative zone (+'ve ordinate) or in a region where the cubic model indicates that the quadratic solution "overestimates" the lamina strength (-'ve ordinate). In this latter case, appropriate safety factors could then be applied to the stress analysis.

8.0 CONCLUDING REMARKS

(a) The quadratic failure criterion with $F_{12} = 0$ provides accurate estimates of failure stresses for the woven graphite/epoxy plain weave fabric prepreg investigated in this report. Since a similar conclusion was reported in Ref. 4 for a Kevlar/epoxy fabric of satin weave construction, it is conjectured that the quadratic model probably provides quite reasonable strength estimates for orthotropic woven fabrics.

(b) The cubic failure criterion has been re-cast into an operationally easier form, providing the engineer with design curves that can be applied to laminates fabricated from orthotropic woven fabric prepregs. In the form presented, no interaction strength tests are required, although recourse to the quadratic model and the

principal strength parameters is necessary. However, insufficient test data exists at present to generalize this approach for all prepreg constructions and its use must be restricted to the generic materials and configurations investigated to-date.

REFERENCES

1. Tennyson, R. C., Nanyaro, A. P. and Wharram, G. E., "Application of the Cubic Polynomial Strength Criterion to the Failure Analysis of Composite Materials", J. Composite Materials Supplement, Vol. 14, 1980.
2. Tennyson, R. C. and Elliott, W. G., "Failure Analysis of Composite Laminates Including Biaxial Compression", NASA CR 172192, August 1983.
3. Tsai, S. W. and Wu, E. M., "A General Theory of Strength for Anisotropic Materials", J. Composite Materials, Vol. 5, 1971.
4. Tennyson, R. C. and Wharram, G. E., "Development of Failure Criterion for Kevlar/Epoxy Fabric Laminates", NASA CR-172465, Dec. 1984.

Table 1 Plane Stress Failure Model Test Requirements*

Failure Model	Test Requirements
Max. Stress or Strain (1)	0° tension, compression 90° tension, compression 0° or 90° shear
Quadratic (2)	Same as (1), with option to evaluate interaction term F_{12} analytically (using "closure" condition) or with biaxial tension test
Cubic (3)	Same as (1) with requirement to evaluate: F_{12}, F_{112}, F_{122}, F_{166}, F_{266} Minimum requirements: Biaxial tenstion test + 4 constraint eq. Preferable: Biaxial tension, biaxial compression + 2 constraint eq. (see Refs.1,2)

* These hold for an orthotropic material, such as unidirectional prepreg or woven (orthotropic) fabric. In the latter case 0° and 90° refer to warp and fill directions, respectively.

Table 2. Graphite Weave 5208-WT300 Tension Test Results

Table 2(a) 0^{o} (Warp Direction)

Test #	$\sigma_{1\ ult}$(ksi)	$E_{11}(10^6$ psi)	ν_{12}	$\varepsilon_{1\ ult}$(%)
1	70.6	9.71	0.055	0.74
2	66.4	-	-	-
3	59.0	9.93	0.061	0.60
4	65.0	9.75	0.070	0.68
5	66.9	10.30	0.074	0.66
6	66.6	-	-	-
AVERAGE	65.8	9.92	0.065	0.67

Table 2(b) 90^{o} (Fill Direction)

Test #	$\sigma_{2\ ult}$(ksi)	$E_{22}(10^6$psi)	ν_{21}	$\varepsilon_{2\ ult}$(%)
1	69.7	-	-	-
2	71.7	-	-	-
3	71.8	10.12	0.069	0.72
4	65.4	10.26	0.062	0.65
5	71.5	10.23	0.065	0.71
6	70.0	-	-	-
AVERAGE	70.0	10.20	0.065	0.69

Table 3 Graphite Weave 5208-WT300 Compression Test Results

Table 3(a) 0^{o} (Warp Direction)

Test #	$\sigma_{1\ ult}$(ksi)	$E_{11}(10^6$ psi)	$\varepsilon_{1\ ult}$(%)
1	65.3	7.77	0.84
2	42.5*	7.83	0.46*
3	58.6	7.31	0.80
4	67.5	7.33	0.96
5	73.3	7.87	0.95
AVERAGE	66.2	7.62	0.89

*Not included in average

Table (3b) 90^{o} (Fill Direction)

Test #	$\sigma_{2\ ult}$ (ksi)	$E_{22}(10^6$ psi)	$\varepsilon_{2\ ult}$(%)
1	51.4	8.92	0.62
2	82.3	7.62	1.13
3	57.3	8.45	0.71
4	68.1	8.30	0.82
5	76.3	7.89	1.00
AVERAGE	67.1	8.24	0.86

Table 4 Graphite Weave 5208-WT300 Torsion Test Results

Table 4(a) 0^{o} Warp Direction)

Test #	τ_{ult}(ksi)	$G_{12}(10^6$ psi)	γ_{ult}(%)
1	17.5	0.75	6.33
2	16.6	0.74	5.31
3	17.1	0.74	5.59
4	17.5	0.72	6.15
AVERAGE	17.2	0.74	5.85

Table 4(b) 90^{o} (Fill Direction)

Test #	τ_{ult}(ksi)	$G_{12}(10^6$ psi)	γ_{ult}(%)
1	17.6	0.76	5.82
2	17.6	0.76	5.38
3	17.2	0.74	5.33
4	16.7	0.73	5.29
AVERAGE	17.3	0.75	5.45

Table 5 Summary of Graphite Weave 5208-WT300 Material Properties

Property	0^o(Warp)	90^o(Fill)	Average Value
$E_{Tension}(10^6$ psi)	9.92	10.20	10.06
Poisson Ratio	0.065	0.065	0.065
$\varepsilon_{ult_T}(\%)$	0.67	0.69	0.68
σ_{ult_T}(ksi)	65.8	70.0	67.9
$E_{compression}(10^6$ psi)	7.62	8.24	7.93
$\varepsilon_{ult_C}(\%)$	0.89	0.86	0.87
σ_{ult_C}(ksi)	66.2	67.1	66.7
$G_{12}(10^6$ psi)	0.74	0.75	0.74
$\gamma_{ult}(\%)$	5.85	5.45	5.65
τ_{ult}(ksi)	17.2	17.3	17.2

Table 6 Graphite Weave 5208-WT300 Interaction Test Results

Test #	Ply Angle (degrees)	Test Description	Failure Pressure(PSI)	σ_1 ult (ksi)	σ_2 ult (ksi)	τ_{ult} (ksi)	ε_1 ult (%)	ε_2 ult (%)	γ_{ult} (%)
1	90	P	1718	57.3	28.6	0.	0.72	0.27	0.
2	90	P	1747	58.2	29.1	0.	0.82	0.27	0.
3	0	P	1743	29.1	58.1	0.	0.27	0.83	0.
4	90	TT	-	0.	43.1	16.8	0.	0.48	5.43
5	0	TT	-	35.1	0.	17.5	0.34	0.	4.31
6	0	TT	-	33.6	0.	18.4	-	-	-
7	±45	P	1850	45.6	46.9	15.4	-	-	-
8	±45	P	1855	45.8	47.0	15.5	-	-	-
9	±30	P	2008	27.2	73.2	6.1	-	-	-

Note: P = Internal Pressure Test

TT = Combined Tension-Torsion Test

Table 7 Strength Reduction of Internal Pressure Tests Due to Material Overlap

Test #	Ply Angle (degrees)	Failure Pressure (psi)	Average Failure Pressure-Non Overlap (psi)	Ratio $\frac{\text{Non Overlap}}{\text{Overlap}}$
10	0	1681	1743	1.037
11	0	1673	1743	1.042
12	0	1582	1743	1.102
13	90	1668	1733	1.039
14	90	1631	1733	1.063
15	45	1739	1853	1.066
AVERAGE				1.058

Table 8 Adjusted Failure Stresses for Overlap Failures

Test #	Ply Angle (degrees)	Test Description	Adjusted Stresses σ_1(ksi)	σ_2(ksi)	σ_6(ksi)	Adjusted Stresses σ_1(ksi)	σ_2(ski)	σ_6(ksi)
10	0	P	28.0	56.0	0.	29.6	59.3	0.
11	0	P	27.9	55.8	0.	29.5	59.0	0.
12	0	P	26.4	52.7	0.	27.9	55.8	0.
13	90	P	55.6	27.8	0.	58.8	29.4	0.
14	90	P	54.4	27.2	0.	57.5	28.8	0.
15	45	P	42.9	44.0	14.5	45.4	46.6	15.3
16	0	PC	-25.3	54.4	0.	-26.8	57.5	0.

Note: P = Internal Pressure Test

PC = Combined Internal Pressure and Axial Compression

Table 9 Summary of Strength Parameters for Graphite Weave Material 5208-WT300

Principal Strength Parameters

$$F_1 = 9.183 \times 10^{-8} \text{ psi}^{-1}$$
$$F_2 = -6.174 \times 10^{-7} \text{ psi}^{-1}$$
$$F_6 = 0.0$$
$$F_{11} = 2.296 \times 10^{-10} \text{ psi}^{-2}$$
$$F_{22} = 2.129 \times 10^{-10} \text{ psi}^{-2}$$
$$F_{66} = 3.380 \times 10^{-9} \text{ psi}^{-2}$$

Interaction Terms

$$F_{12} = F_{122} = F_{112} = 0$$
$$F_{166} = -1.097 \times 10^{-14} \text{ psi}^{-3}$$
$$F_{266} = -8.845 \times 10^{-15} \text{ psi}^{-3}$$
$$-\tfrac{1}{2}(F_{11}F_{22})^{\frac{1}{2}} = -1.105 \times 10^{-10} \text{ psi}^{-2}$$

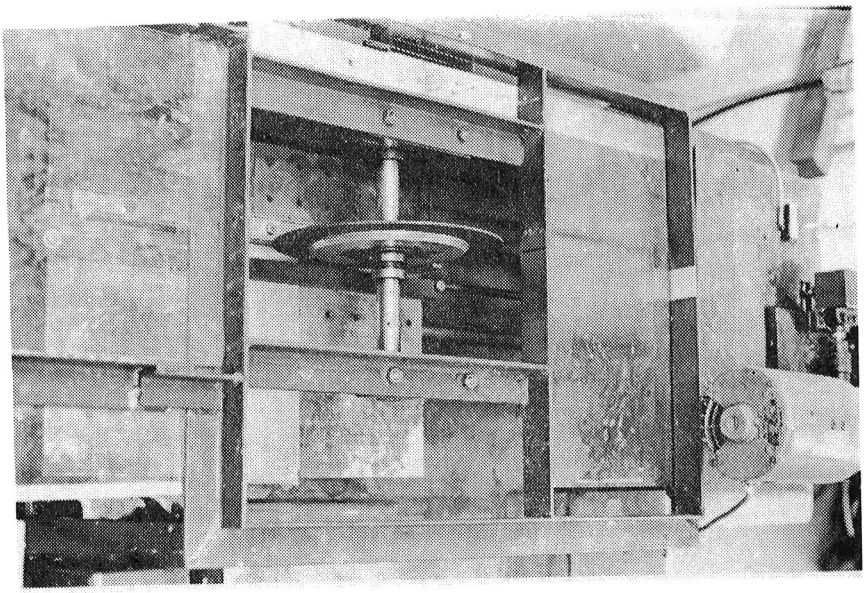

Fig. 1 FLAT SPECIMEN ABRASIVE WHEEL CUTTING APPARATUS

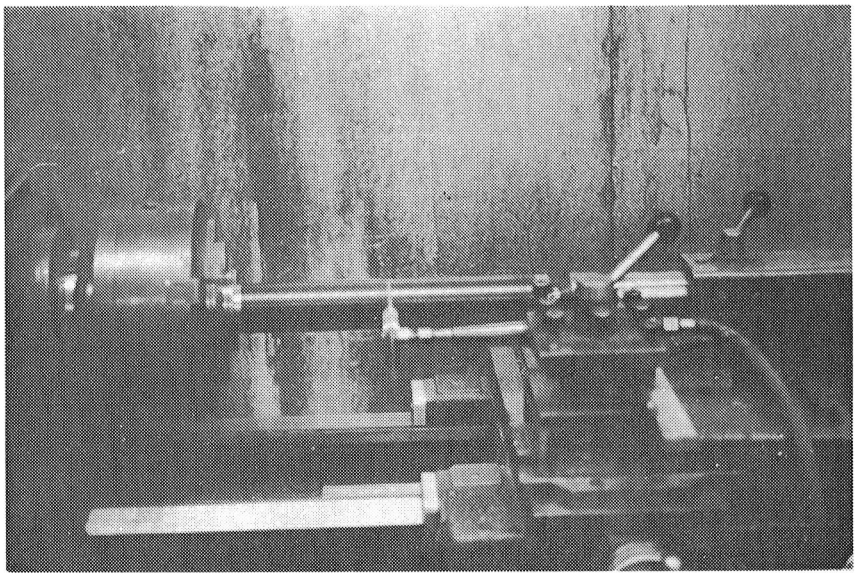

Fig. 2 TUBE CUTTING APPARATUS

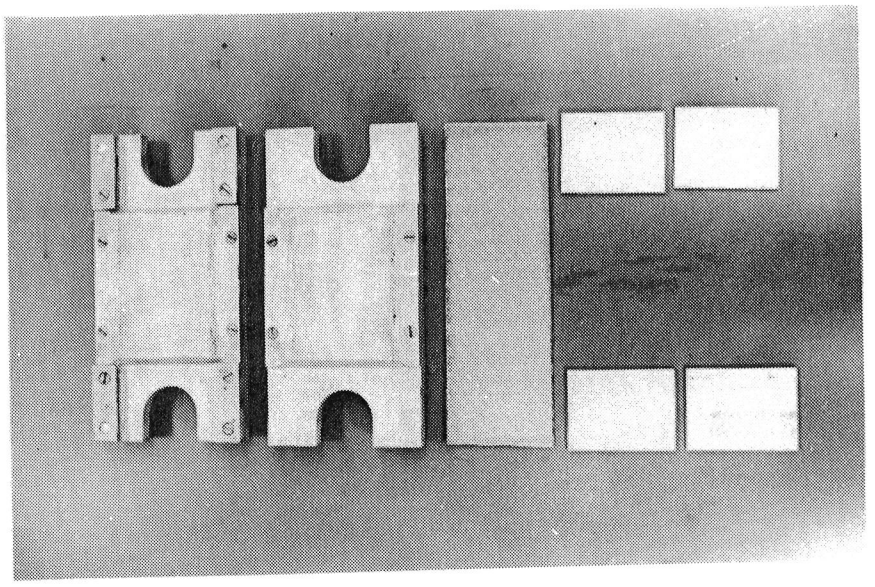

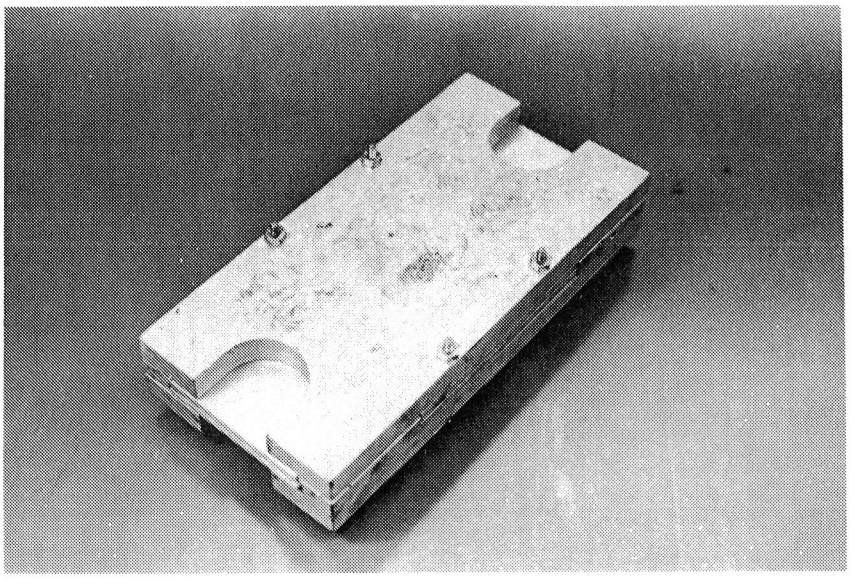

Fig. 3 TENSION SAMPLE and END GRIP FIXTURE

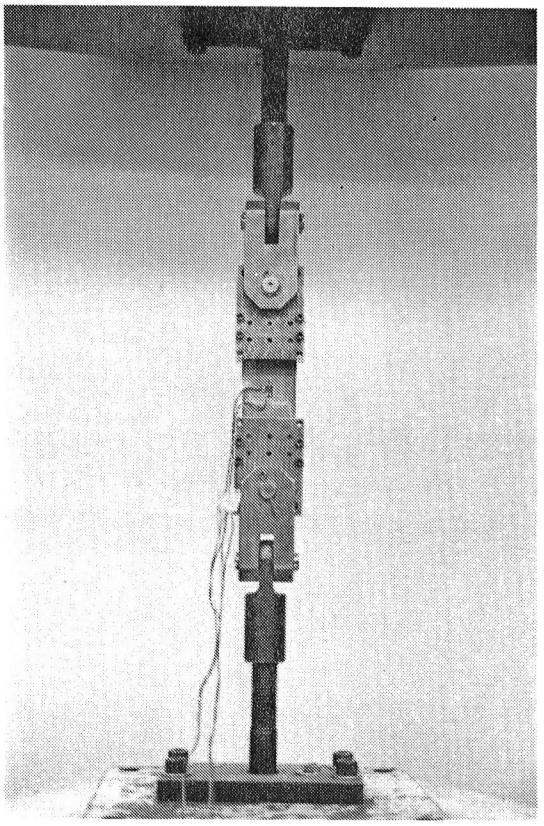

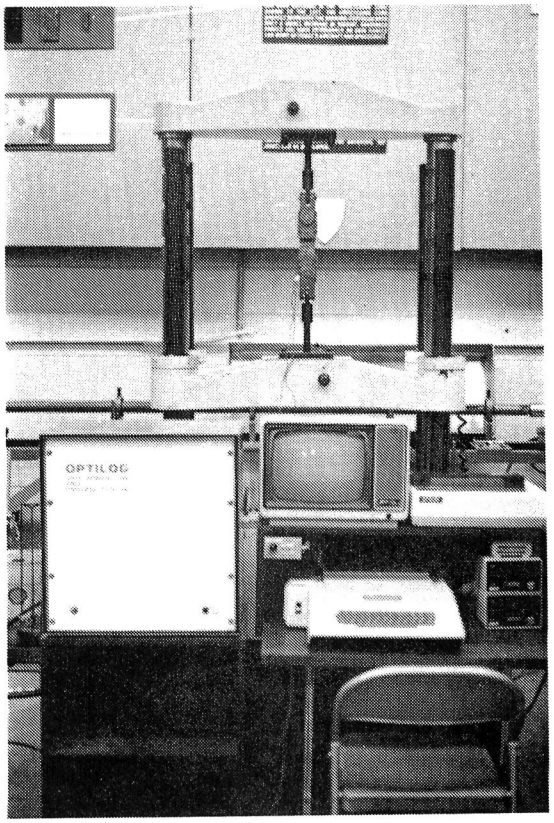

Fig. 4
TENSION GRIPS IN
TINIUS OLSEN
TESTING MACHINE

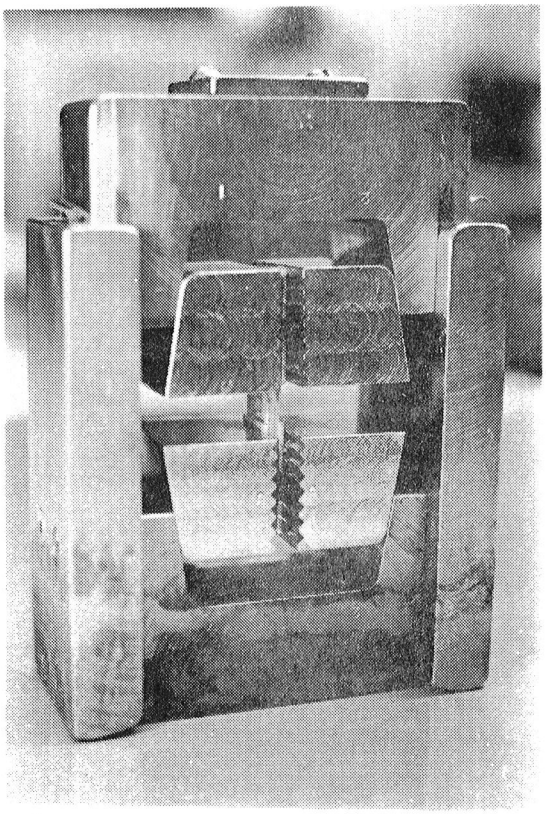

Fig. 5
II TRI – TYPE
COMPRESSION GRIPS

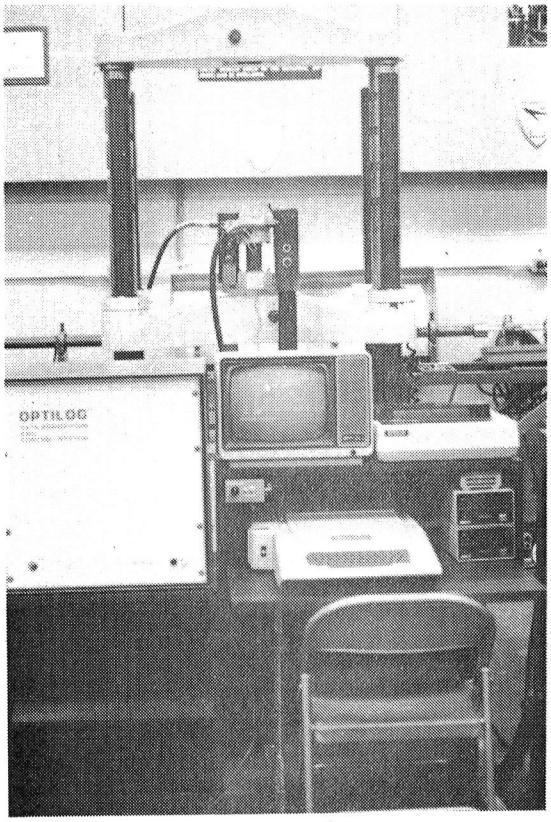

Fig. 6
TORSION TEST
FACILITY

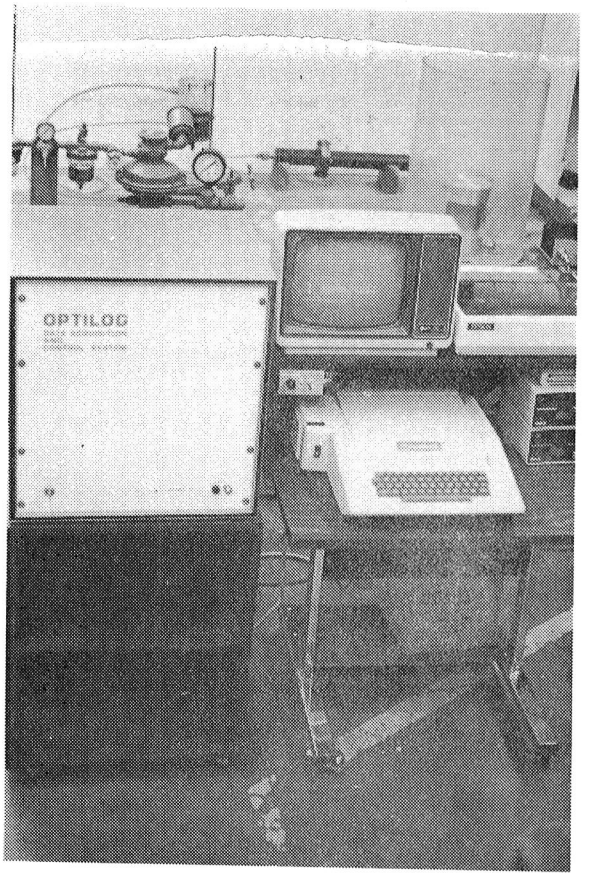

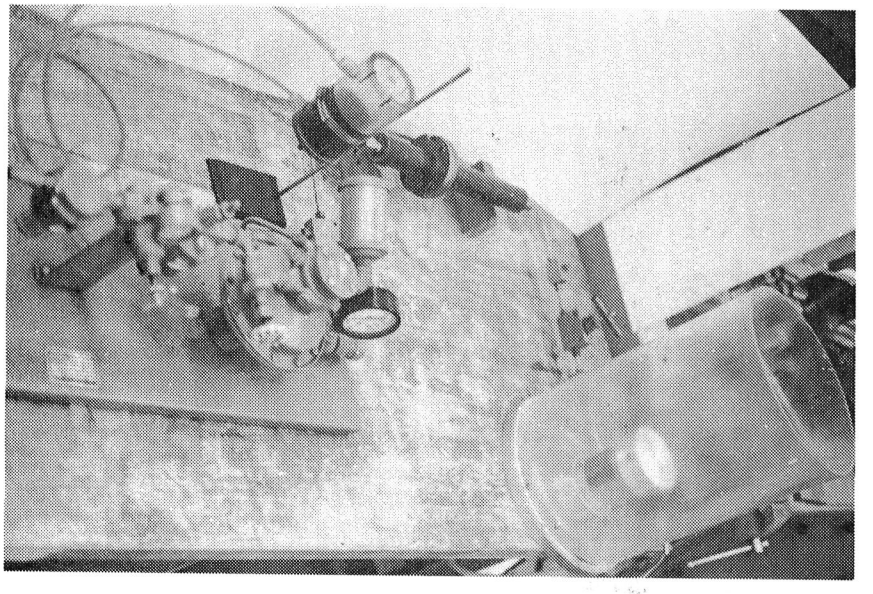

Fig. 7 PRESSURE TEST FACILITY WITH DATA ACQUISITION SYSTEM

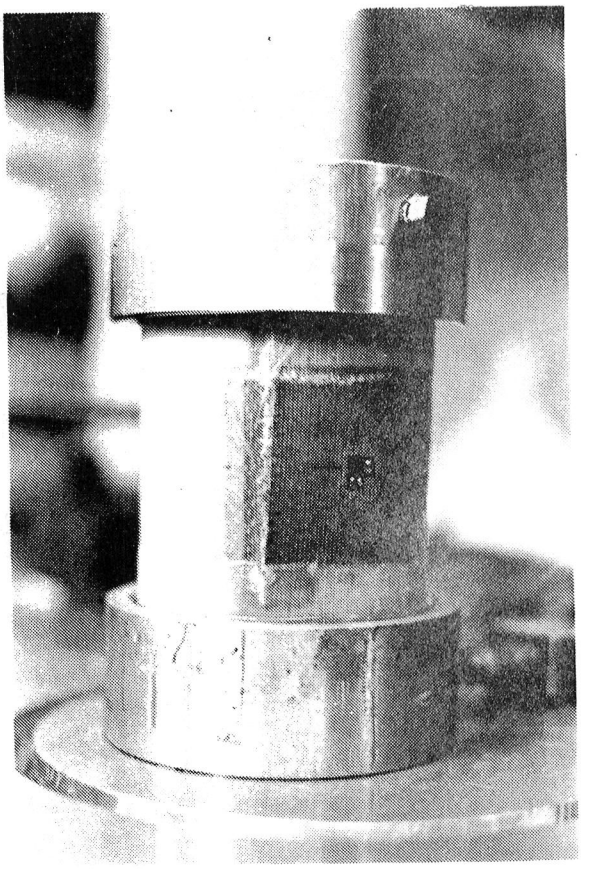

Fig. 8 PRESSURE TEST SPECIMEN

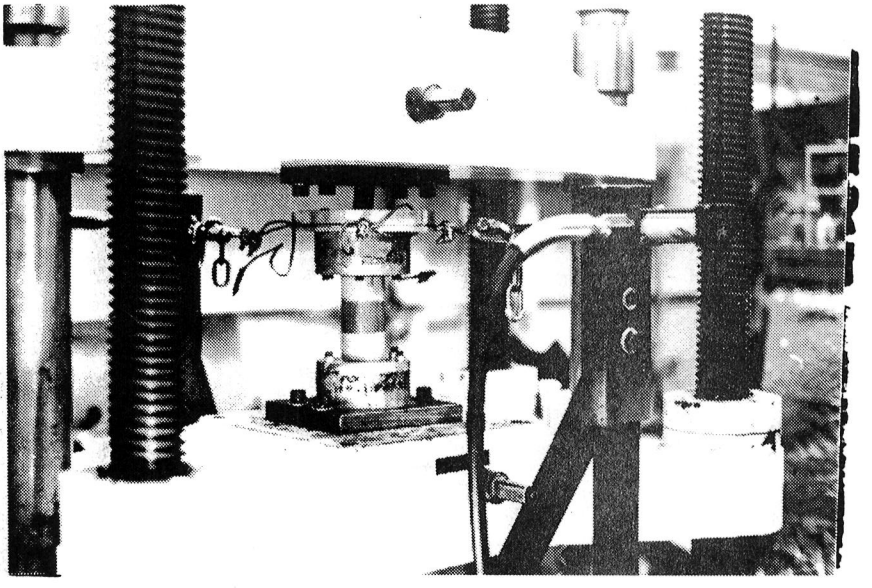

Fig. 9 TENSION - TORSION TEST APPARATUS

Fig. 10 Graphite Weave Tension Test

0 Deg. Sample #1

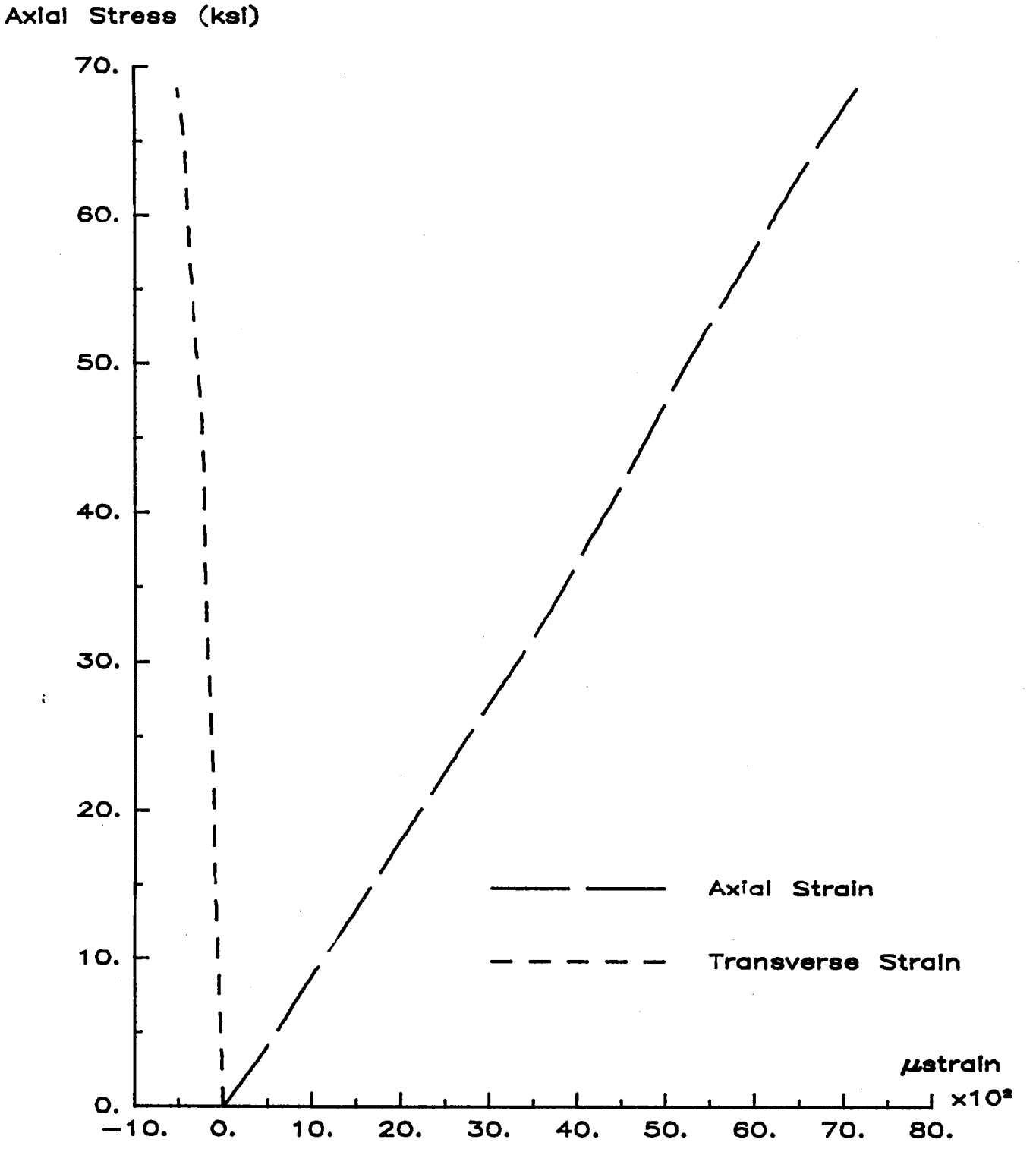

Fig. 11 Graphite Weave Tension Test

90 Deg. Sample #3

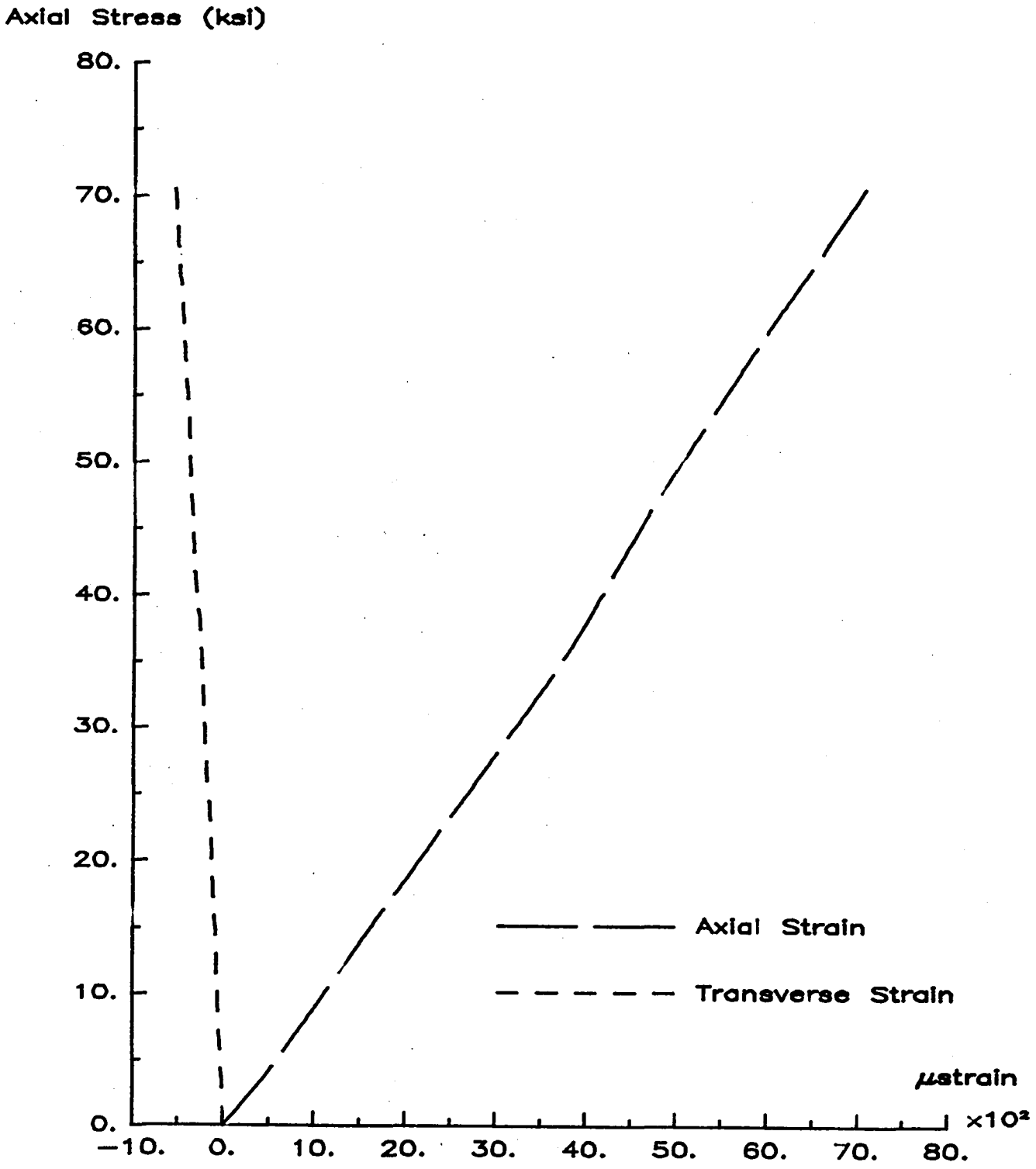

Fig. 12 Graphite Weave Compression Test

0 Deg. Sample #5

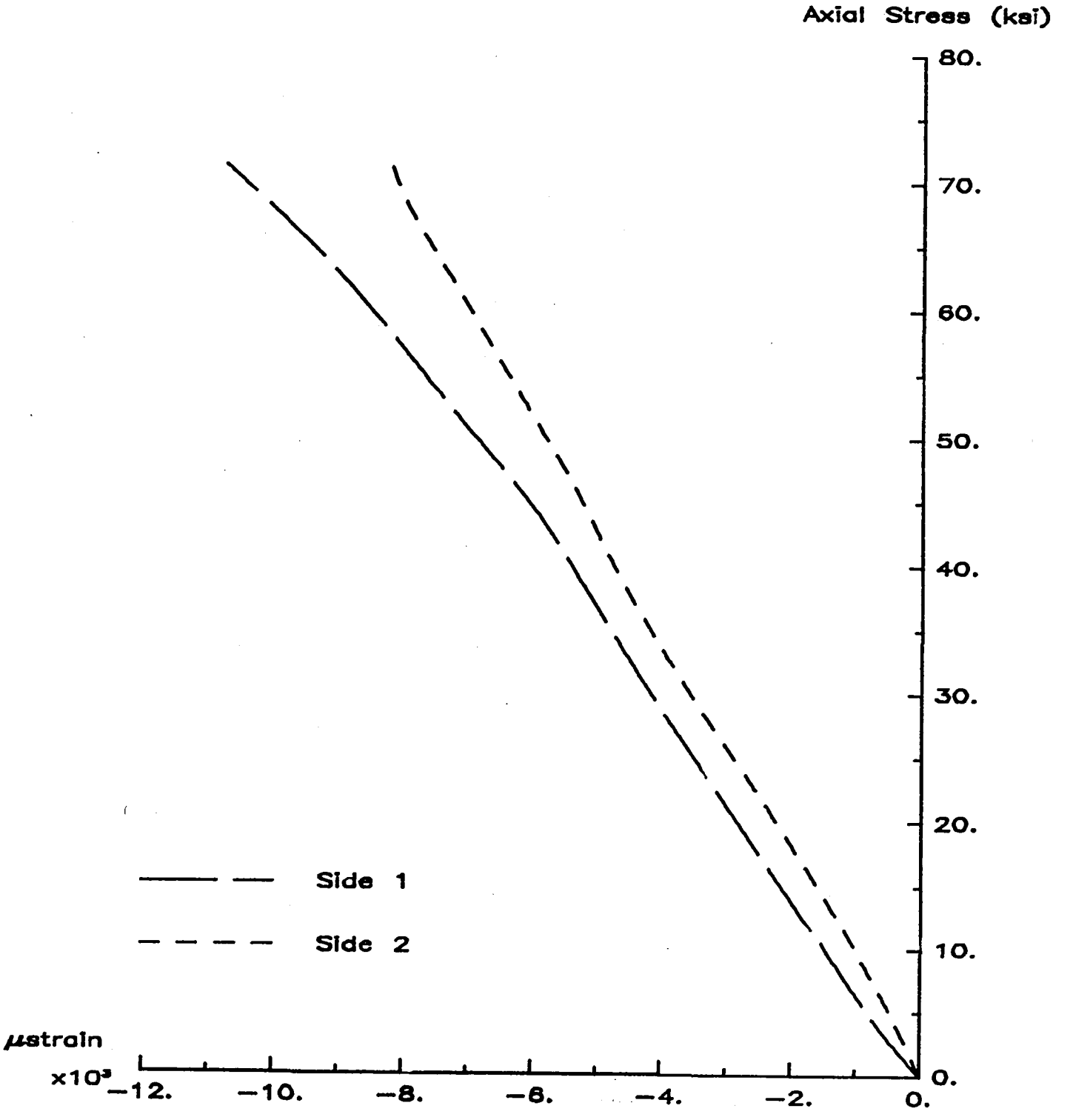

Fig. 13 Graphite Weave Compression Test

90 Deg. Sample #5

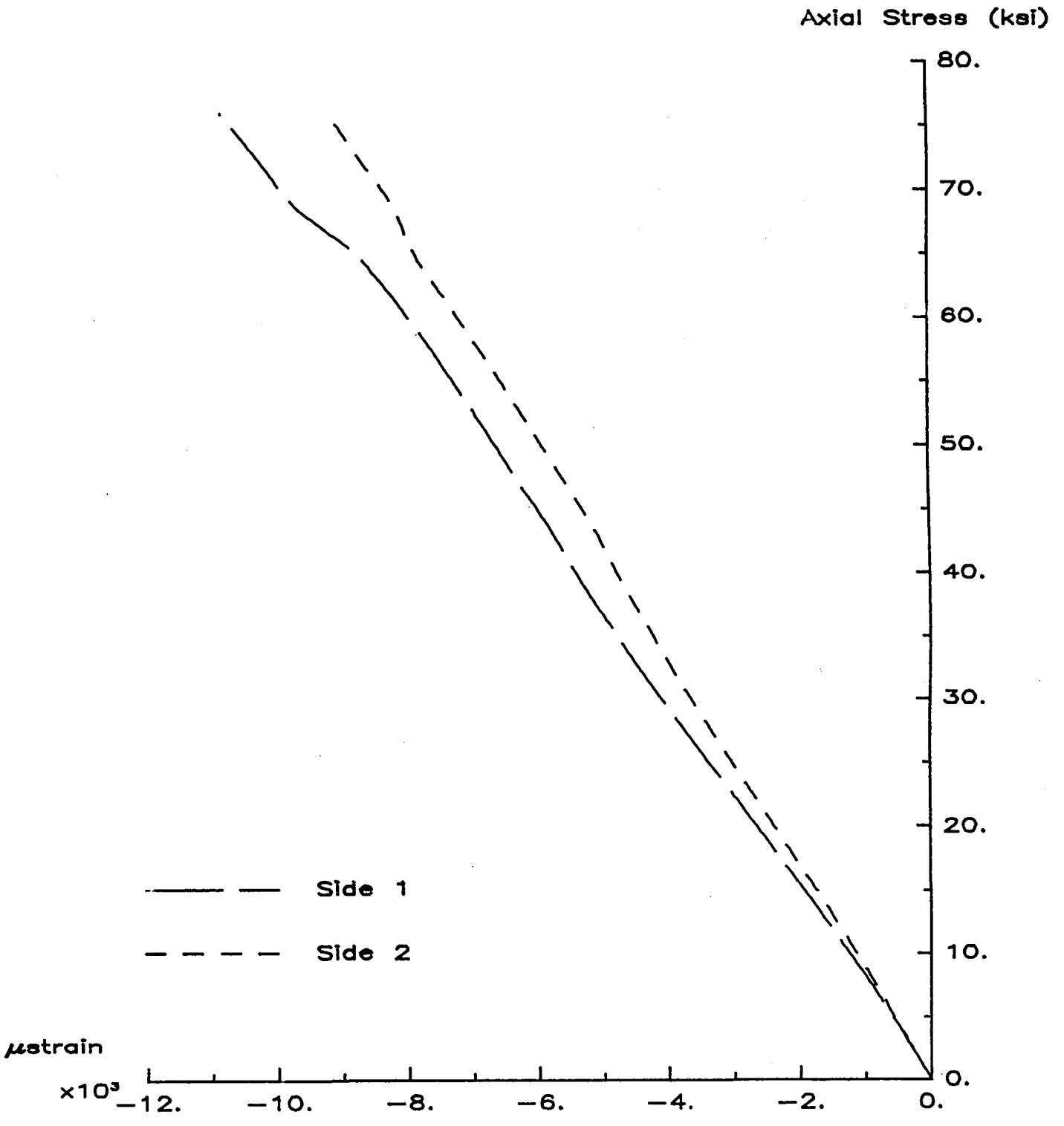

Fig. 14 Graphite Weave Torsion Test

0 Deg. Sample #3

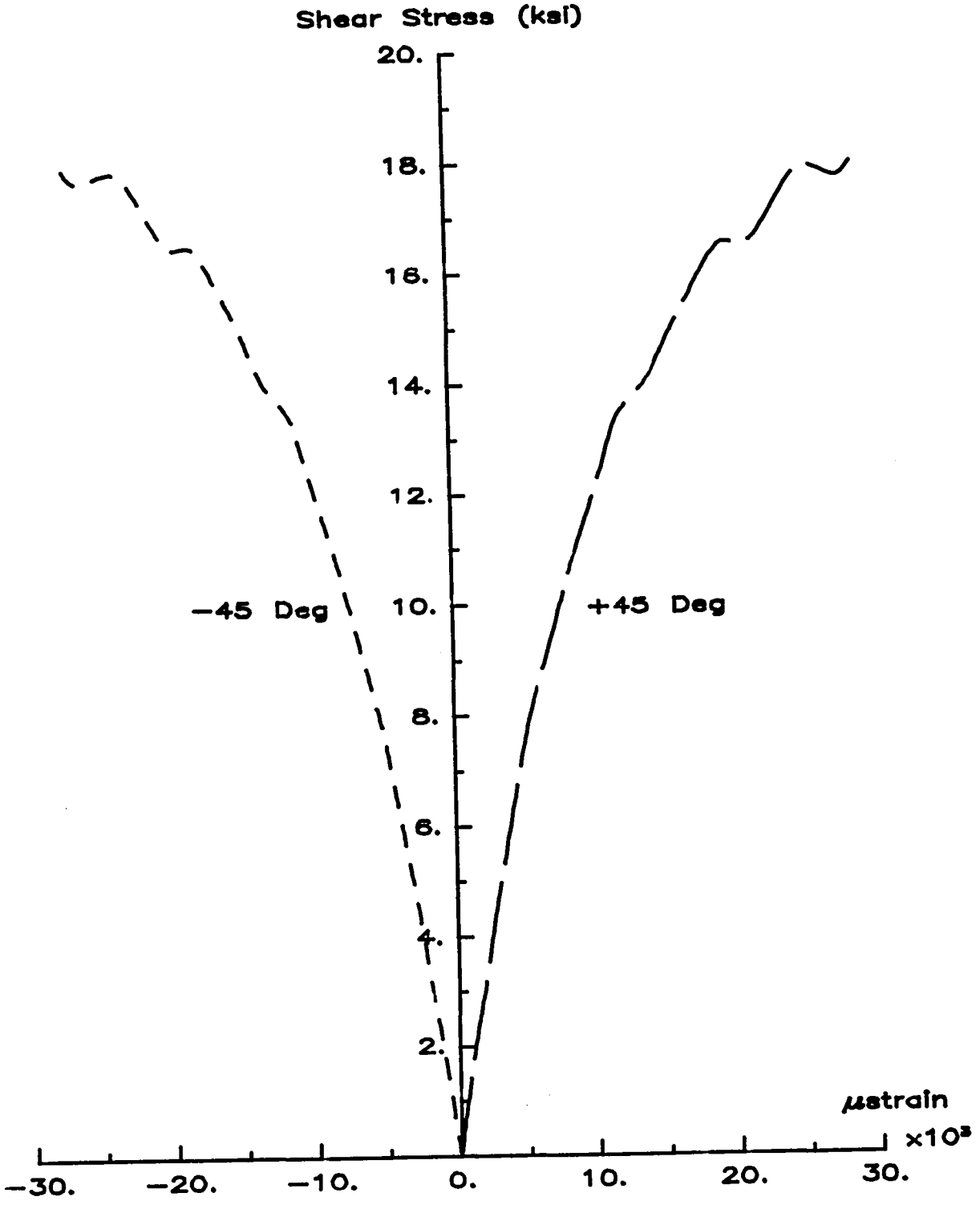

Fig. 15 Graphite Weave Torsion Test

90 Deg. Sample #2

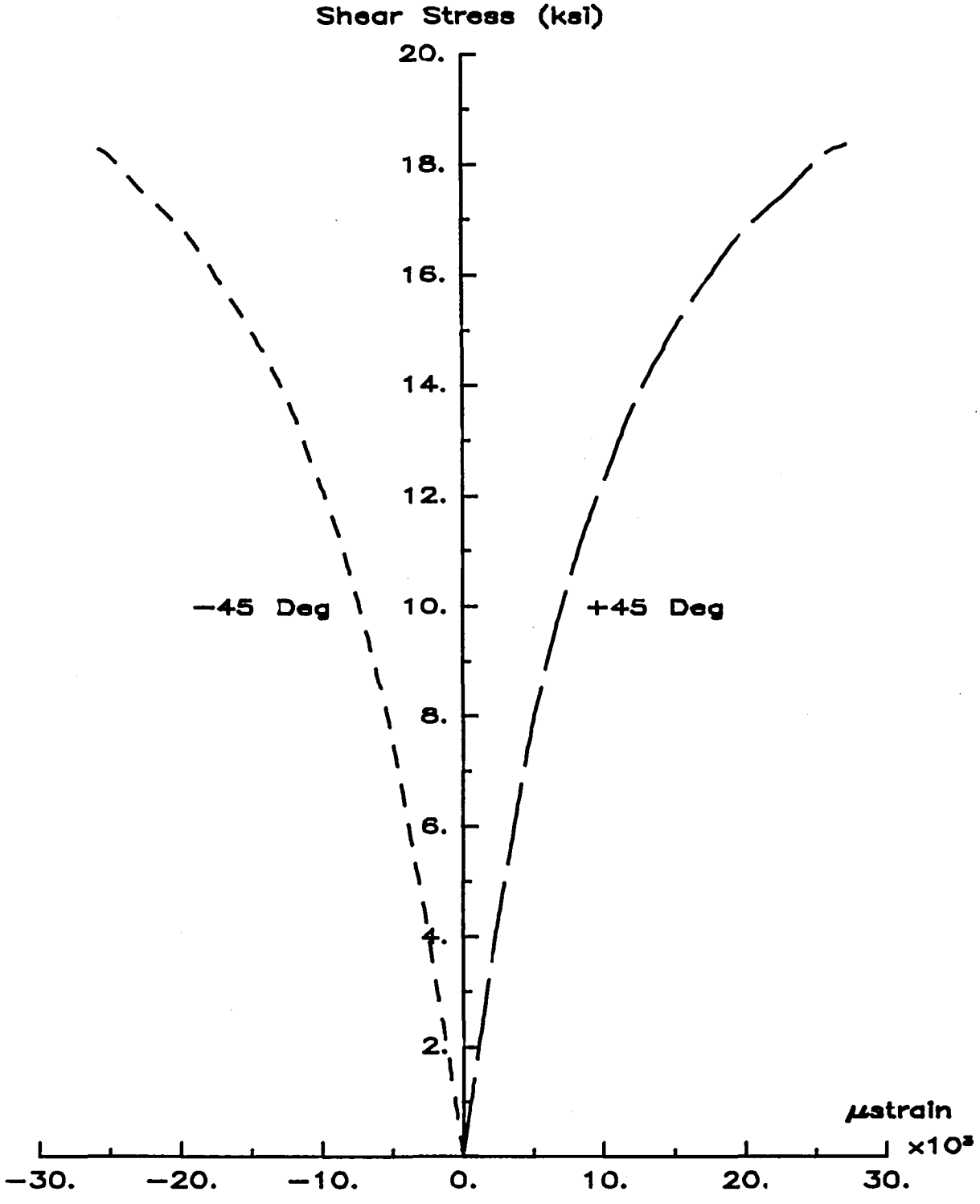

Fig. 16 Graphite Weave Failure Surface

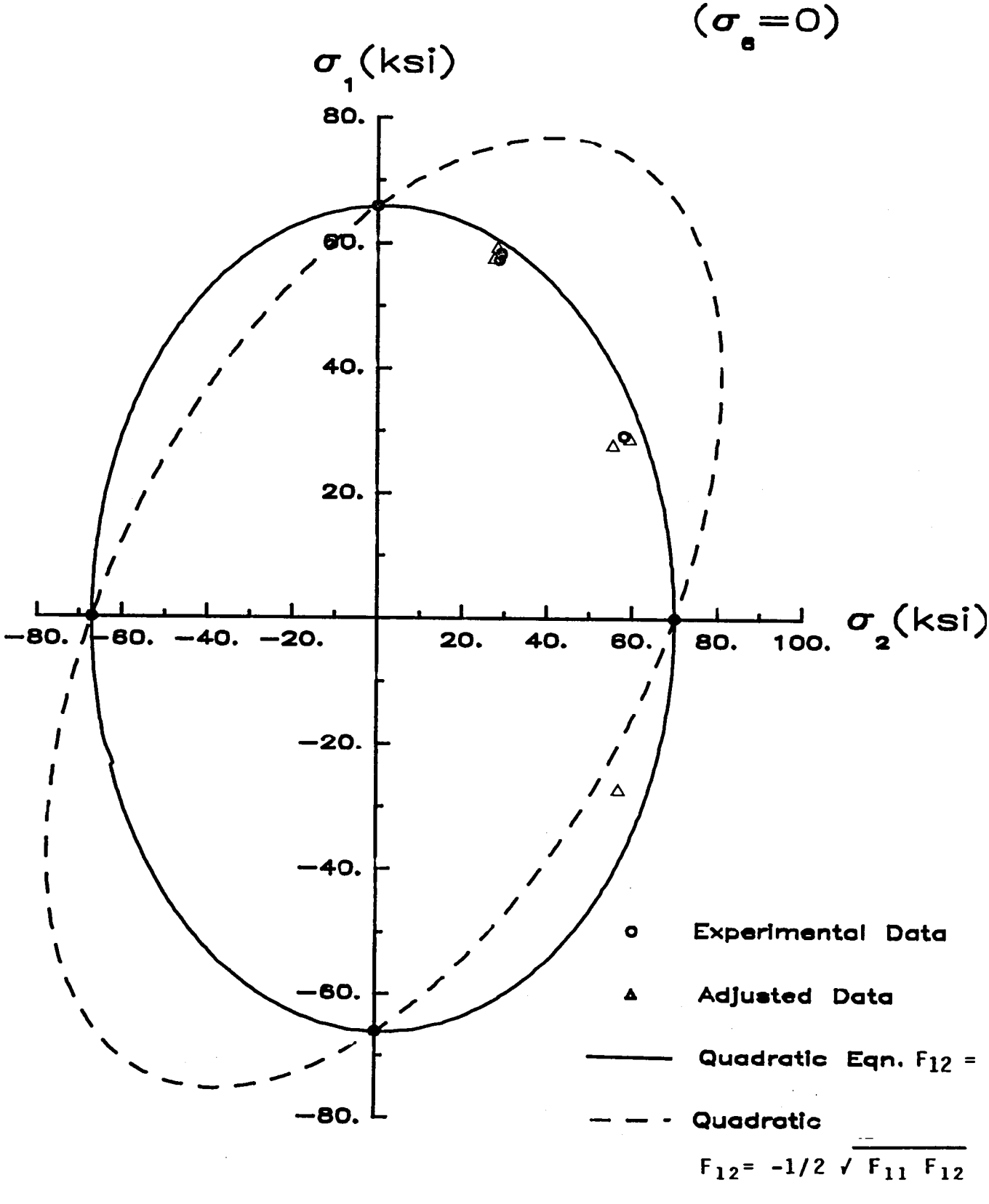

Fig. 17 Graphite Weave Failure Surface

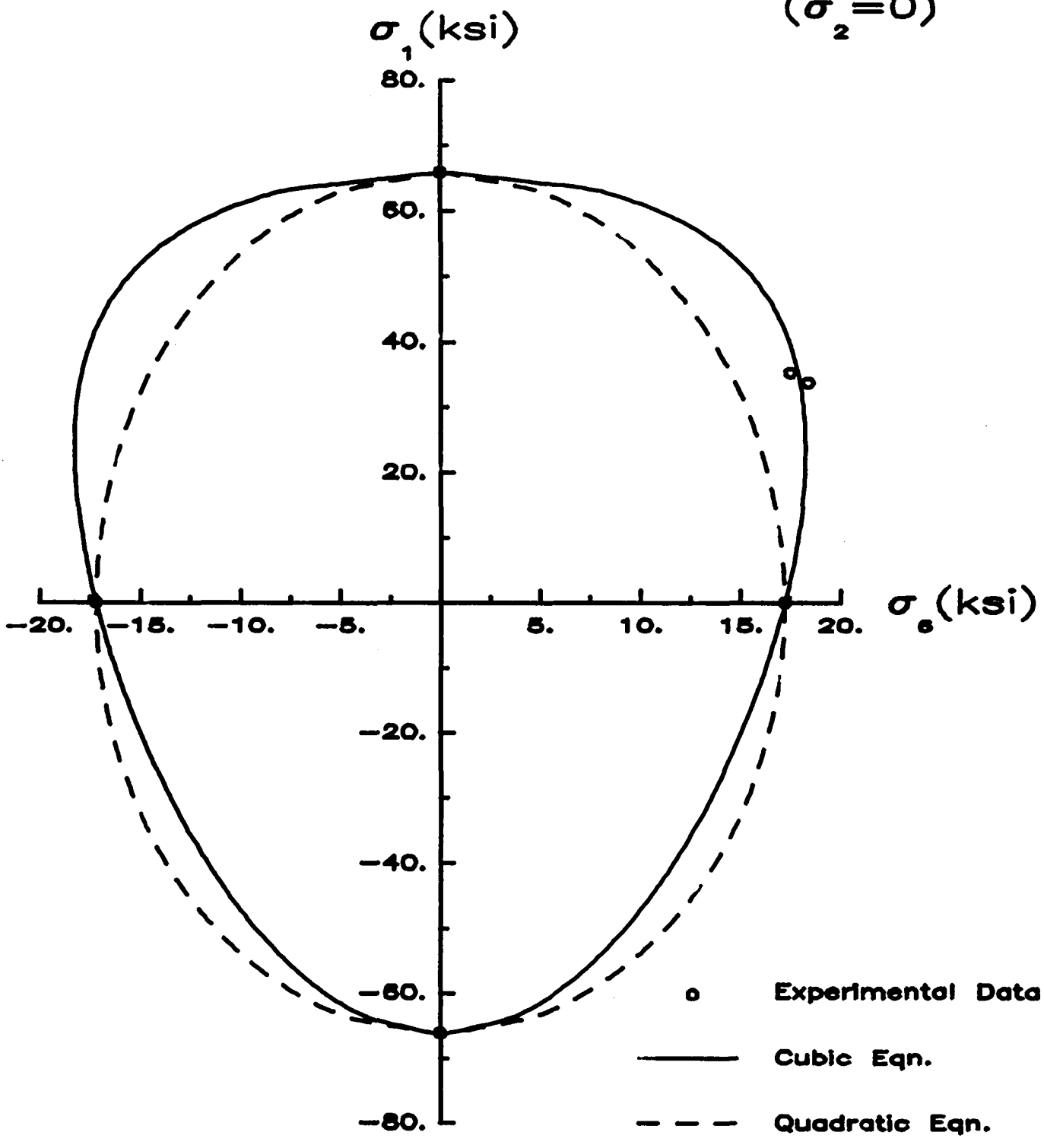

Fig. 18 Graphite Weave Failure Surface

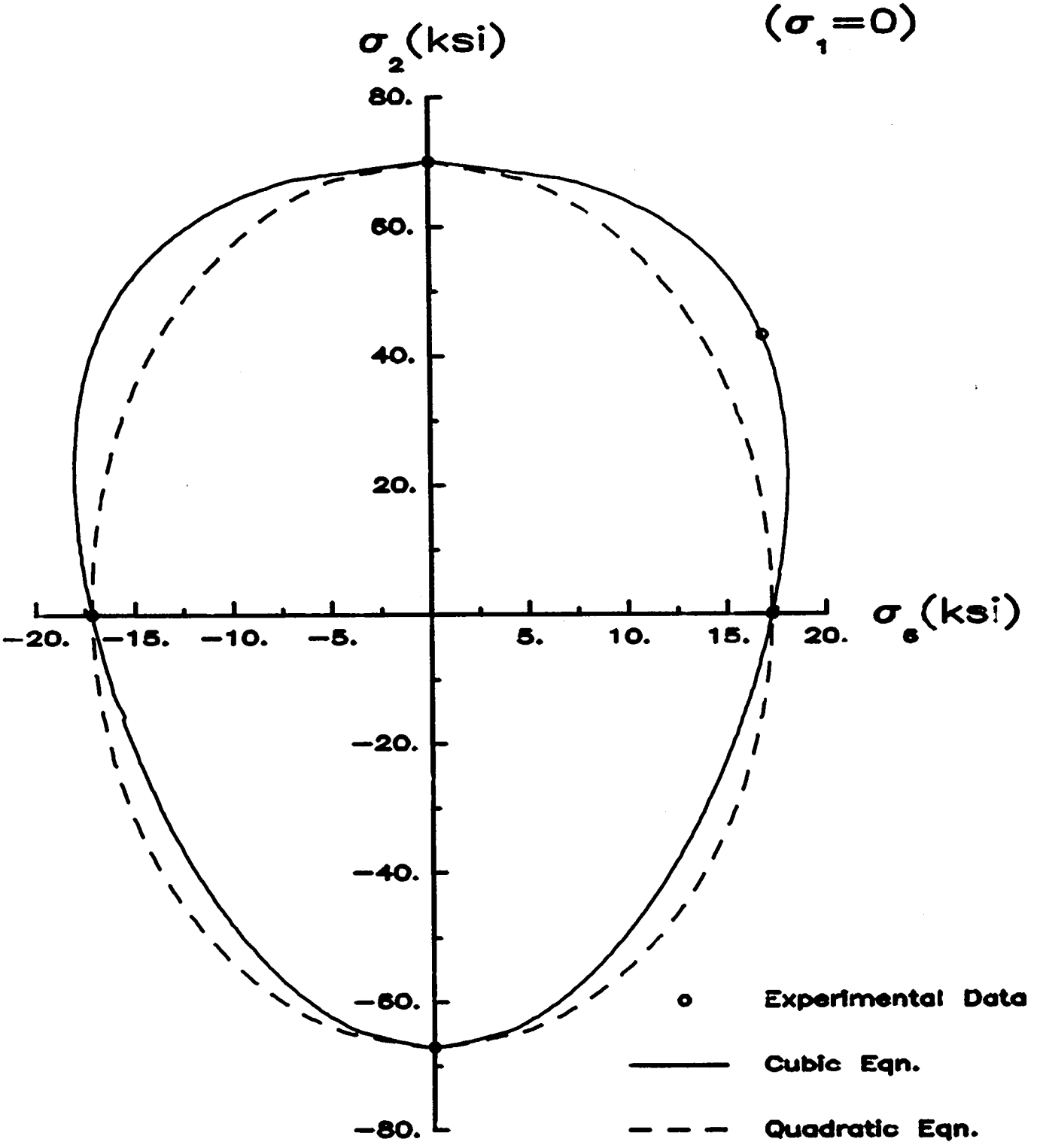

Fig. 19 Failure Pressure vs Ply Angle
Symmetric Balanced $\pm$ Ⓜ Tubes
Graphite Weave Material

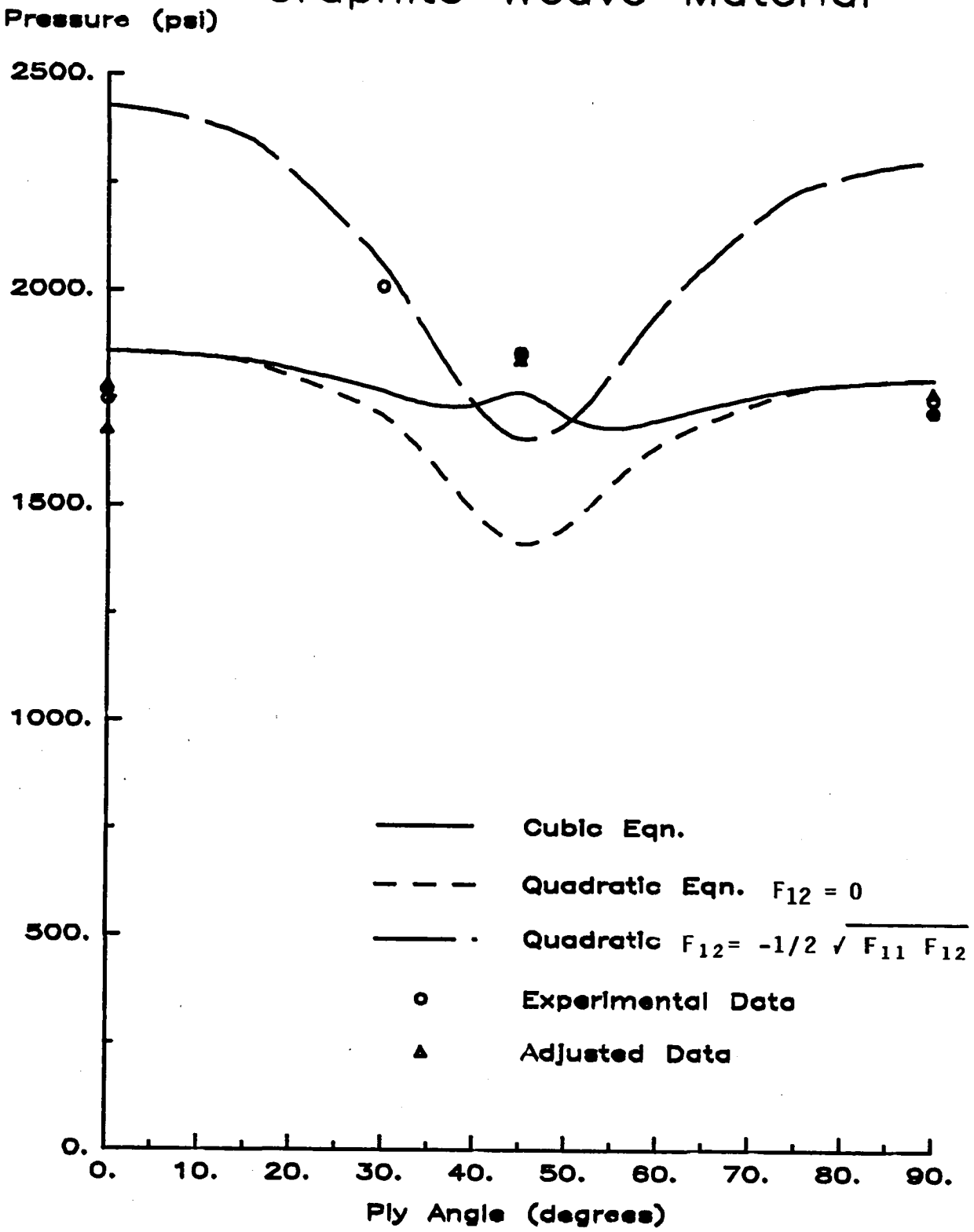

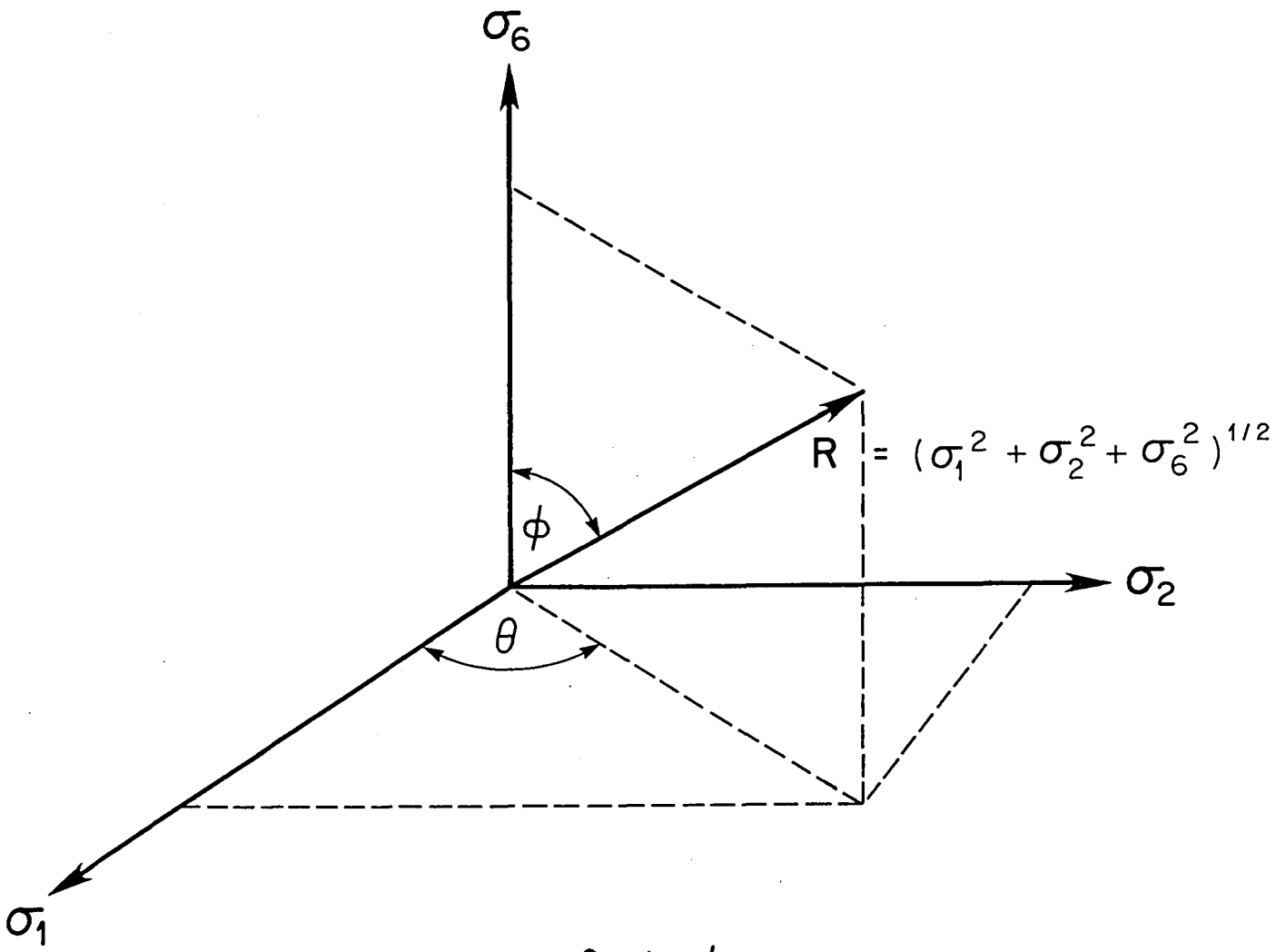

$$\sigma_1 = R \cos\theta \sin\phi$$
$$\sigma_2 = R \sin\theta \sin\phi$$
$$\sigma_6 = R \cos\phi$$

Fig. 20 RESOLUTION OF LOAD VECTOR R IN STRESS SPACE

Fig. 21 Design Factors for Correcting Quadratic Model Strength Predictions for Graphite Weave Material

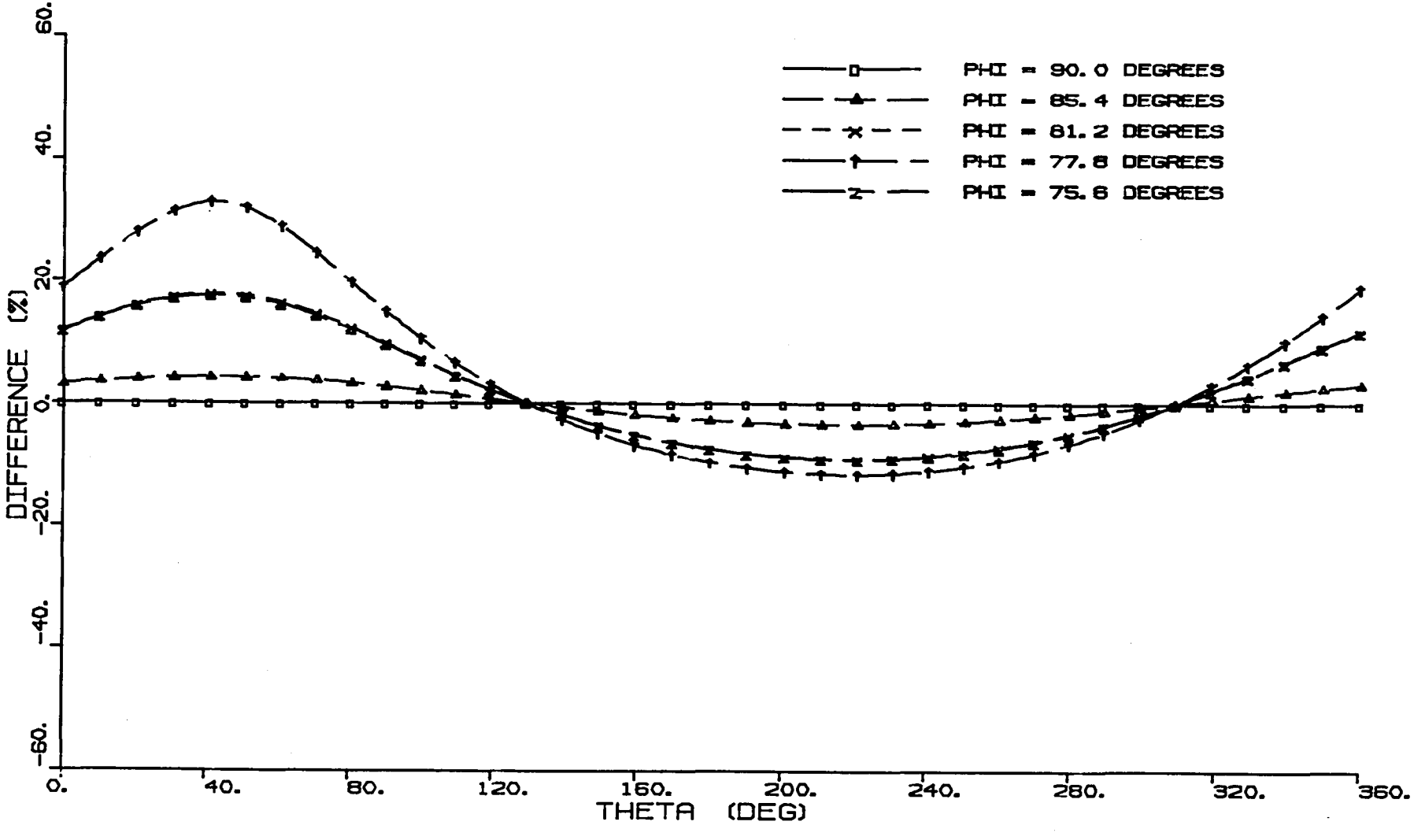

1. Report No.	2. Government Accession No.	3. Recipient's Catalog No.
NASA CR-172547		

4. Title and Subtitle	5. Report Date
Evaluation of Failure Criterion for Graphite/Epoxy Fabric Laminates	February 1985
	6. Performing Organization Code
7. Author(s)	8. Performing Organization Report No.
R. C. Tennyson and G. E. Wharram	10. Work Unit No.
9. Performing Organization Name and Address University of Toronto Institute for Aerospace Studies Toronto, Ontario, Canada	11. Contract or Grant No. NSG-7409
	13. Type of Report and Period Covered Contractor Report 8/83-12/84
12. Sponsoring Agency Name and Address National Aeronautics and Space Administration Washington, DC 20546	14. Sponsoring Agency Code 505-42-23-03

15. Supplementary Notes
Langley Technical Monitor: Donald J. Baker
Interim Report

16. Abstract

This report describes a continued effort on the development and application of the tensor polynomial failure criterion for composite laminate analysis. In particular, emphasis in this report is given to the fabrication and testing of Narmco Rigidite 5208-WT300, a plain weave fabric of Thornel 300 Graphite fibers impregnated with Narmco 5208 Resin. The quadratic-failure criterion with $F_{12}=0$ provides accurate estimates of failure stresses for the Graphite/Epoxy investigated.

The cubic failure criterion has been recast into an operationally easier form, providing the engineer with design curves that can be applied to laminates fabricated from orthotropic woven fabric pregregs. In the form presented, no interaction strength tests are required, although recourse to the quadratic model and the principal strength parameters is necessary. However, insufficient test data exist at present to generalize this approach for all prepreg constructions, and its use must be restricted to the generic materials and configurations investigated to date.

17. Key Words (Suggested by Author(s))
Composite Structures
Failure Analysis
Laminates
Modulus of Elasticity
Tsi-Wu Criterion

18. Distribution Statement
Unclassified-unlimited
Subject Category 24

19. Security Classif. (of this report)	20. Security Classif. (of this page)	21. No. of Pages	22. Price
Unclassified	Unclassified	45	A03

For sale by the National Technical Information Service, Springfield, Virginia 22161

LANGLEY RESEARCH CENTER
3 1176 01351 7991

DO NOT REMOVE SLIP FROM MATERIAL

Delete your name from this slip when returning material to the library.

NAME	DATE	MS
~~Ecol Edit Technician~~	~~July 31~~	~~ILC~~

NASA Langley (Rev. Dec. 1991) RIAD N-75